


# Spinor *F*= 1 Bose-Einstein condensates loaded in two types of radially-periodic potentials with spin-orbit coupling

Ji-Guo Wang(王继国), Yue-Qing Li(李月晴), Han-Zhao Tang(唐翰昭), and Ya-Fei Song(宋亚飞)
**Citation:**Chin. Phys. B, 2021, 30 (**10**): 106701. DOI: 10.1088/1674-1056/ac1411
Journal homepage: http://cpb.iphy.ac.cn; http://iopscience.iop.org/cpb

**What follows is a list of articles you may be interested in**

---

## Polaron and molecular states of a spin-orbit coupled impurity in a spinless Fermi sea

Hong-Hao Yin(尹洪浩), Tian-Yang Xie(谢天扬), An-Chun Ji(纪安春), and Qing Sun(孙青)
Chin. Phys. B, 2021, 30 (**10**): 106702. DOI: 10.1088/1674-1056/ac1b85

## Bose-Einstein condensates under a non-Hermitian spin-orbit coupling

Hao-Wei Li(李浩伟) and Jia-Zheng Sun(孙佳政)
Chin. Phys. B, 2021, 30 (**6**): 066702. DOI: 10.1088/1674-1056/abd7e4

## Ground-state phases and spin textures of spin–orbit-coupled dipolar Bose–Einstein condensates in a rotating toroidal trap

Qing-Bo Wang(王庆波), Hui Yang(杨慧), Ning Su(苏宁), and Ling-Hua Wen(文灵华)
Chin. Phys. B, 2020, 29 (**11**): 116701. DOI: 10.1088/1674-1056/abbbe8

## Spatiotemporal Bloch states of a spin-orbit coupled Bose-Einstein condensate in an optical lattice

Ya-Wen Wei(魏娅雯), Chao Kong(孔超), Wen-Hua Hai(海文华)
Chin. Phys. B, 2019, 28 (**5**): 056701. DOI: 10.1088/1674-1056/28/5/056701

## Phase diagram and collective modes in Rashba spin–orbit coupled BEC: Effect of in-plane magnetic field

Dong Dong, Zou Xu-Bo, Guo Guang-Can
Chin. Phys. B, 2015, 24 (**7**): 076701. DOI: 10.1088/1674-1056/24/7/076701

---

# Spinor $F = 1$ Bose–Einstein condensates loaded in two types of radially-periodic potentials with spin–orbit coupling*

Ji-Guo Wang(王继国)[1,2,†], Yue-Qing Li(李月晴)[1,2], Han-Zhao Tang(唐翰昭)[1,2], and Ya-Fei Song(宋亚飞)[1,2]

[1] *Department of Mathematics and Physics, Shijiazhuang TieDao University, Shijiazhuang* 050043, *China*
[2] *Institute of Applied Physics, Shijiazhuang TieDao University, Shijiazhuang* 050043, *China*

(Received 11 May 2021; revised manuscript received 19 June 2021; accepted manuscript online 14 July 2021)

We consider two-dimensional spinor $F = 1$ Bose–Einstein condensates in two types of radially-periodic potentials with spin–orbit coupling, *i.e.*, spin-independent and spin-dependent radially-periodic potentials. For the Bose–Einstein condensates in a spin-independent radially-periodic potential, the density of each component exhibits the periodic density modulation along the azimuthal direction, which realizes the necklacelike state in the ferromagnetic Bose–Einstein condensates. As the spin-exchange interaction increases, the necklacelike state gradually transition to the plane wave phase for the antiferromagnetic Bose–Einstein condensates with larger spin–orbit coupling. The competition of the spin-dependent radially-periodic potential, spin–orbit coupling, and spin-exchange interaction gives rise to the exotic ground-state phases when the Bose–Einstein condensates in a spin-dependent radially-periodic potential.

**Keywords:** spinor Bose–Einstein condensates, spin–orbit coupling, radially-periodic potential

**PACS:** 67.85.−d, 05.30.Jp, 71.70.Ej, 03.75.Mn **DOI:** 10.1088/1674-1056/ac1411

## 1. Introduction

Spinor Bose–Einstein condensates (BECs) had been experimental realized in $Na^{23}$ and $Rb^{87}$ using dipole optical trap by the Tin-Lun Ho and Tetsuo Ohmi groups in 1998.[1,2] Three spin degrees of freedom are shown in spinor BECs, which corresponding to the three hyperfine spin states with $m_F = -1$, 0, 1 for $F = 1$. Within the mean-field theory, spinor $F = 1$ BECs show a rich variety of magnetic phenomena. The ferromagnetic state, antiferromagnetic state or polar state are exhibited in spin-1 BECs, the types of the ground-state phases are depended on the spin-exchange interaction. Many interesting topological excitations of the spin vortex, monopoles, two-dimensional (2D) skyrmion and three-dimensional (3D) skyrmion are proposed from these phases.[3–11] In addition, different types of solitons have been given rise to much attention in spin-1 BECs, such as the dark soliton, bright soliton, bright-dark soliton complexes, gap soliton and rogue wave.[12–20]

The realization of spin–orbit coupling (SOC) in spinor gases in experiment[21] opens fascinating questions about the physics of spin–orbit coupled ultracold gases, it has aroused the theoretical and experimental attentions on spin–orbit coupled BECs rapidly.[22–31] Two distinct phases, *i.e.*, single plane-wave state and density-stripe state are found in a homogeneous spin–orbit coupled spin-1/2 BECs[32] and the quantum states with Skyrmion lattice patterns are emerged[25] in spin–orbit coupled spin-1/2 BECs loaded in a harmonic trap. Three kinds of striped phases with qualitatively different behaviors in the modulations of the density profiles in a homogeneous spin–orbit coupled spin-1 BECs depended on the antiferromagnetic interaction or ferromagnetic interaction.[33–36] Recently, spin–orbit coupled spinor BECs in the different periodic potentials, like the toroidal trap, spin-dependent periodic potential and radially-periodic potential are investigated, which results in many exotic ground-state phases and solitons.[37–46]

In this paper, we consider 2D spin–orbit coupled spin-1 BECs in two types of radially-periodic potentials, *i.e.*, spin-independent and spin-dependent radially-periodic potentials. For the BECs in a spin-independent radially-periodic potential, the density of each component exhibits the periodic density modulation along the azimuthal direction, which realizes the necklacelike state in the ferromagnetic BECs. As the spin-exchange interaction increases, the necklacelike state gradually transition to the plane wave phase for the antiferromagnetic BECs with larger SOC. The competition of the spin-dependent radially-periodic potential, SOC and spin-exchange interaction gives rise to the exotic ground-state phases when the BECs in a spin-dependent radially-periodic potential.

The paper is organized as follows. In Section 2 we introduce the model of 2D spin–orbit coupled spin-1 BECs in a radially periodic potential. In Section 3 we display the ground-state phases of spin–orbit coupled spin-1 BECs in a spin-independent radially periodic potential in Subsection 3.1 and pin-dependent radially periodic potential in Subsection 3.2. A brief summary is included in Section 4.

*Project supported by the National Natural Science of China (Grant Nos. 11904242 and 12004264) and the Natural Science Foundation of Hebei Province, China (Grant Nos. A2019210280 and A2019210124).

†Corresponding author. E-mail: wangjiguo@stdu.edu.cn

© 2021 Chinese Physical Society and IOP Publishing Ltd 

## 2. Model and Hamiltonian

We consider spin–orbit coupled spin-1 BECs loaded in the radially-periodic potential. The Hamiltonian can be described by the mean-field approximation, it is

$$H = \int \mathrm{d}\boldsymbol{r}\Psi_j^\dagger \left[-\frac{\hbar^2}{2m}\nabla^2 + V(\boldsymbol{r}) + \upsilon_{\mathrm{soc}}\right]\Psi_j + \int \mathrm{d}\boldsymbol{r}\left(\frac{1}{2}c_0 n^2 + \frac{1}{2}c_2|\boldsymbol{F}|^2\right), \tag{1}$$

where $\Psi_j$ $(j=0,\pm1)$ is the three-component spinor wave functions of the atoms in the spin state $|F=1,m_F=j\rangle$. The total atomic density $n = n_1 + n_0 + n_{-1} = \sum_j |\Psi_j|^2$ and the total particle number $N = \int \Psi^\dagger \Psi \mathrm{d}^2\boldsymbol{r}$ with $\Psi = [\Psi_{-1}(r), \Psi_0(r), \Psi_1(r)]^{\mathrm{T}}$. The density-density and spin-exchange interactions are $c_0 = \frac{4}{3}\hbar^2\pi(2a_2+a_0)/m$ and $c_2 = \frac{4}{3}\hbar^2\pi(a_2-a_0)/m$, respectively. They can be adjusted by the $s$-wave scattering length $a_s$ $(s=0,2)$ for total spin $0,2$. The spin density $\boldsymbol{F} = (F_x,F_y,F_z) = (\Psi^\dagger\hat{F}_x\Psi, \Psi^\dagger\hat{F}_y\Psi, \Psi^\dagger\hat{F}_z\Psi)$, where $\widehat{F}$ is $3\times3$ matrices,

$$\hat{F}_x = \frac{1}{\sqrt{2}}\begin{pmatrix} 0 & 1 & 0 \\ 1 & 0 & 1 \\ 0 & 1 & 0 \end{pmatrix},$$
$$\hat{F}_y = \frac{\mathrm{i}}{\sqrt{2}}\begin{pmatrix} 0 & -1 & 0 \\ 1 & 0 & -1 \\ 0 & 1 & 0 \end{pmatrix},$$
$$\hat{F}_z = \begin{pmatrix} 1 & 0 & 0 \\ 0 & 0 & 0 \\ 0 & 0 & -1 \end{pmatrix}. \tag{2}$$

The SOC effect $\upsilon_{\mathrm{soc}} = -\mathrm{i}\hbar\gamma(\hat{F}_x\partial_y - \hat{F}_y\partial_x)$ with strength $\gamma$. The external potential $V(r)$ is

$$V(\boldsymbol{r}) = \frac{m}{2}\omega^2\boldsymbol{r}^2 + V_1(\boldsymbol{r}), \tag{3}$$

where $\omega$ is the harmonic trap frequency, and $V_1(\boldsymbol{r})$ is the radially-periodic potential. Here, spin–orbit coupled spin-1 BECs loaded in two types of radially-periodic potentials are discussed, *i.e.*, spin-independent or spin-dependent radially-periodic potential. The spin-independent radially-periodic potential is $V_1(\boldsymbol{r}) = V_0\cos^2(\pi\boldsymbol{r})$. The spin-dependent radially-periodic potential is $V_1(\boldsymbol{r}) = V_0\cos^2(\pi\boldsymbol{r}+\delta)$, where $\delta=0$ for the $m_F=0$ component and $\delta=\pi/2$ for the $m_F=\pm1$ components.

## 3. Spin–orbit coupled spin-1 BECs in the radially-periodic potentials

We discuss the ground-state phases of spin–orbit coupled spin-1 BECs loaded in spin-independent and spin-dependent radially-periodic potentials in Subsection 3.1 and Subsection 3.2, respectively. Three dimensionless coupled time-dependent Gross–Pitaevskii (GP) equations are formulated that from $\mathrm{i}\hbar(\partial\Psi_j/\partial t) = \left(\delta E/\delta\Psi_j^*\right)$,

$$\begin{aligned}
\mathrm{i}\frac{\partial\Psi_{-1}}{\partial t} &= \left(-\frac{1}{2}\nabla^2 + V(\boldsymbol{r})\right)\Psi_{-1} + (c_0 n - c_2 F_z)\Psi_{-1} \\
&\quad + \frac{c_2}{\sqrt{2}}F_+\Psi_0 + \frac{1}{\sqrt{2}}(-\mathrm{i}\partial_y + \partial_x)\Psi_0, \\
\mathrm{i}\frac{\partial\Psi_0}{\partial t} &= \left(-\frac{1}{2}\nabla^2 + V(\boldsymbol{r})\right)\Psi_0 + (c_0 n)\Psi_0 + \frac{c_2}{\sqrt{2}}F_-\Psi_{-1} \\
&\quad + \frac{c_2}{\sqrt{2}}F_+\Psi_1 \\
&\quad + \frac{1}{\sqrt{2}}\left[(-\mathrm{i}\partial_y - \partial_x)\Psi_{-1} + (-\mathrm{i}\partial_y + \partial_x)\Psi_1\right], \\
\mathrm{i}\frac{\partial\Psi_1}{\partial t} &= \left(-\frac{1}{2}\nabla^2 + V(\boldsymbol{r})\right)\Psi_1 + (c_0 n + c_2 F_z)\Psi_1 \\
&\quad + \frac{c_2}{\sqrt{2}}F_-\Psi_0 + \frac{1}{\sqrt{2}}(-\mathrm{i}\partial_y - \partial_x)\Psi_0,
\end{aligned} \tag{4}$$

where $F_\pm = F_x \pm \mathrm{i}F_y$. The length ($x$ and $y$) is normalized by $l = \sqrt{\hbar/(m\omega)}$. The time ($t$), SOC strength ($\gamma$), and interaction ($c_0$, $c_2$) are scaled by $\omega^{-1}$, $l\omega$, and $\hbar\omega l^3/N$, respectively.

We obtain the ground-state phases by using the time-splitting Fourier pseudospectral method with the imaginary-time propagation, *i.e.*, $t \to -\mathrm{i}t$.[47,48] The wave function in Eq. (4) can be written as $\Psi_j(\boldsymbol{r},t) = \sum_{k=1}\Psi_{jk}(\boldsymbol{r})\exp(-\mathrm{i}tE_k)$ with the eigenvalue $E_k$. After each iteration, each eigenfunction is decayed by $\exp(-\mathrm{i}tE_k)$, the returned wave function eigenvalue becomes lower and lower, it tends to the ground-state wave function, which lead to the proportion of the ground-state wave functions becomes larger and larger. When the time is at its limit, the wave functions evolve into the ground-state wave functions. The density–density interaction ($c_0=1000$) and the radially-periodic potential depth ($V_0=20$) are fixed.

### 3.1. Spin-independent radially-periodic potential

We first study on the ground-state phases of spin–orbit coupled spin-1 BECs loaded in a spin-independent radially-periodic potential. For the ferromagnetic BECs with spin-exchange interaction $c_2=-200$, the ground-state density profiles are shown in Fig. 1. The SOC strengths in panels (a)–(d) are $\gamma=0$, 1, 3, and 5, respectively. The columns from left to right are the densities of the $m_F=-1$ component, the $m_F=0$ component, the $m_F=1$ component, the total component, the density difference of the $m_F=1$ component, and the $m_F=-1$ component, the phase of the $m_F=-1$ component and the phase of $m_F=0$ component. The density of each component is uniform distributed in the same ring without SOC, as shown in Fig. 1(a). By considering SOC, we can find that the density of each component exhibits the periodic density modulation along the azimuthal direction. For the small SOC strength $\gamma=1$, the densities of the $m_F=-1$ and the $m_F=1$ components mainly occupy right and left sides, they

are symmetric about the $y$ axis, one can be seen in Figs. 1(b1) and 1(b3), respectively. The density difference of the $m_F = 1$ component and the $m_F = -1$ component in Fig. 1(b4) also shows this character. In Fig. 1(b2), the $m_F = 0$ component density shows a necklacelike state, the numbers of petals double increase as the ring expands one ring outward. With the SOC strength enhances, the phenomena of the periodic density modulation in each component become more obvious. The phases of the $m_F = -1$ and the $m_F = 1$ components exhibit the rotational symmetry with $\gamma = 3$ in Figs. 1(c6) and 1(c7), however, they show the alternating plane waves that propagating on opposite directions along the $y$ axis for larger SOC strength in Figs. 1(d6) and 1(d7), which are similar to the character of the supersolid state.[41,42]

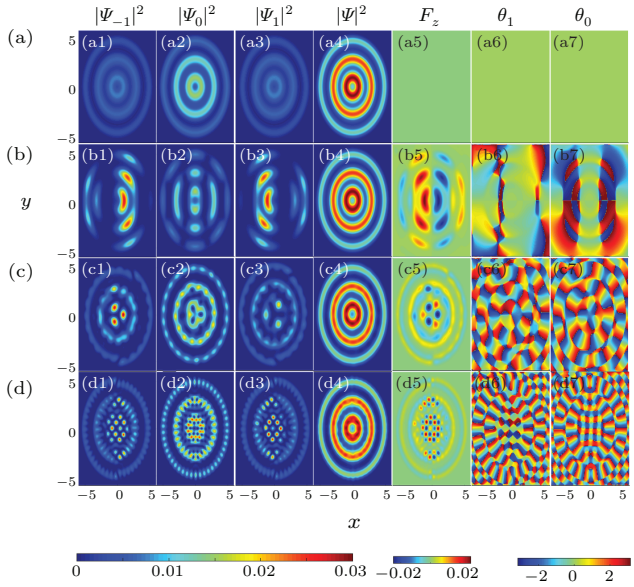



**Fig. 1.** The ground-state density profiles of spin-1 BECs with SOC loaded in a spin-independent radially periodic potential. The SOC strengths in panels (a)–(d) are $\gamma = 0$, 1, 3, and 5, respectively. The columns from left to right are the densities of the $m_F = -1$ component, the $m_F = 0$ component, the $m_F = 1$ component, the total component, the density difference of the $m_F = 1$ component, and the $m_F = -1$ component, the phase of the $m_F = -1$ component and the phase of the $m_F = 0$ component. The spin-exchange interaction $c_2 = -200$.

We also study the ground-state phases of spin–orbit coupled spin-1 BECs loaded in a spin-independent radially-periodic potential with the spin-exchange interactions $c_2 = 200$ in Fig. 2 and $c_2 = 2000$ in Fig. 3. For the antiferromagnetic BECs without SOC, the spin-exchange interaction favors a state with no spontaneous magnetization, the order parameter of the ground-state phase is $\zeta = (1,0,1)^{\mathrm{T}}/\sqrt{2}$, which results in the density of the $m_F = 0$ component is blank and the densities of the $m_F = -1$ and the $m_F = 1$ components are uniform, one can be seen in Fig. 2(a). By considering SOC, the ground-state phases with the SOC strengths $\gamma = 1$, 3, and 5 are respectively shown in panels (b)–(d) in Figs. 2 and 3. The density of atomic gases starts to occupy the $m_F = 0$ component with the small SOC strength. Each component also shows the density periodic modulation along the azimuthal direction in

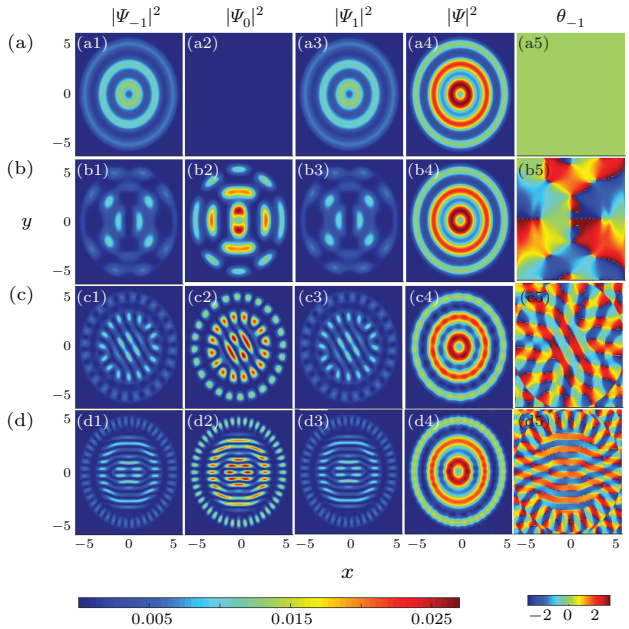



**Fig. 2.** The ground-state density profiles of spin-1 BECs with SOC loaded in a spin-independent radially periodic potential. The SOC strengths in panels (a)–(d) are $\gamma = 0$, 1, 3, and 5, respectively. The columns from left to right are the densities of the $m_F = -1$ component, the $m_F = 0$ component, the $m_F = 1$ component, the total component, and the phase of the $m_F = -1$ component. The spin-exchange interaction $c_2 = 200$.

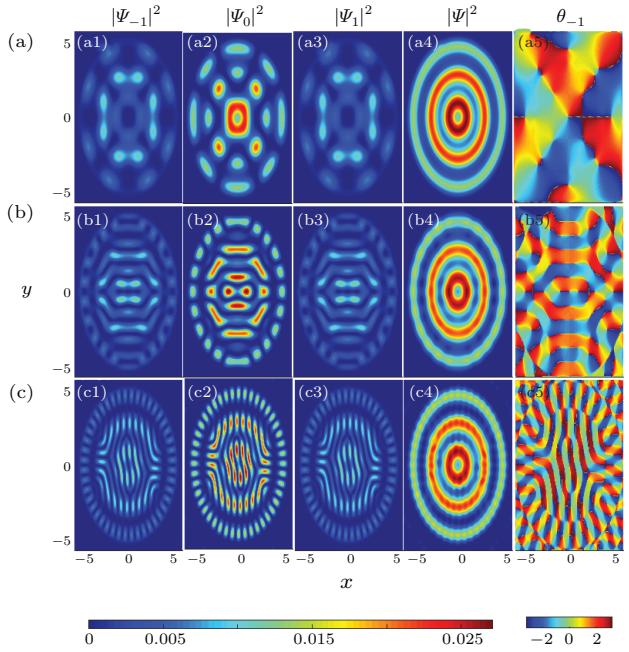



**Fig. 3.** The ground-state density profiles of spin-1 BECs with SOC loaded in a spin-independent radially periodic potential. The SOC strengths in panels (a)–(c) are $\gamma = 1$, 3, and 5, respectively. The columns from left to right are the densities of the $m_F = -1$ component, the $m_F = 0$ component, the $m_F = 1$ component, the total component, and the phase of the $m_F = -1$ component. The spin-exchange interaction $c_2 = 2000$.

Fig. 2(b) with the weak spin-exchange interaction $c_2 = 200$. The densities of the $m_F = -1$ and the $m_F = 1$ components can be self-symmetric, which are different from the ferromagnetic BECs with $\gamma = 1$ in Fig. 1(b). The second inner ring shows square lattice structure in the $m_F = \pm 1$ components and two sets of periodic structures in the $m_F = 0$ component with strong spin-exchange interaction $c_2 = 2000$. For the larger

SOC strength $\gamma = 3$, the ground-state also remains necklace-like structure, however, the rotational symmetry is broken in the innermost ring, the density realizes the plane wave, one can be seen in the phase of the $m_F = -1$ component in Fig. 2(c5). With the spin-exchange interaction increases, the plane wave character becomes more obvious, as shown in Fig. 3(b). In Figs. 2(d) and 3(c), when the SOC strength is increased beyond a critical value, the periodic density modulations along both the radial and the azimuthal directions appears in inner rings of each component.

### 3.2. Spin-dependent radially-periodic potential

We next consider spin–orbit coupled spin-1 BECs loaded in a spin-dependent radially-periodic potential. The ground-state density profiles are shown in Fig. 4 with the different spin-exchange interactions strengths $c_2 = -200$, 200, and 2000 in panels (a)–(c), respectively. The SOC strength $\gamma = 5$. The competition of the spin-dependent radially-periodic potential, SOC and spin-exchange interaction gives rise to the exotic ground-state phases. For the ferromagnetic BECs, the spin-dependent radially-periodic potential and SOC break the translational symmetry of density along one direction, and the translational symmetry along the direction that perpendicular to it is preserved. For the antiferromagnetic BECs, the density of each component shows the ring structure with spin-exchange interaction $c_2 = 200$ in Fig. 4(b). The innermost rings consist of two semicircles in the $m_F = \pm 1$ components, which results in the density of the $m_F = 0$ component is divided into two half arcs. The structure of innermost rings of the total density is similar to the double lung of human organs. An interesting phenomenon in Fig. 4(b5), the phase profile of the $m_F = -1$ component consists of alternating vortices along the opposite directions, which is caused by the spin-dependent radially-periodic potential and SOC. As the spin-exchange interaction increases, the ring structures are broken. The double vortices are shown in the phase profile of the $m_F = -1$ component in Fig. 4(c).

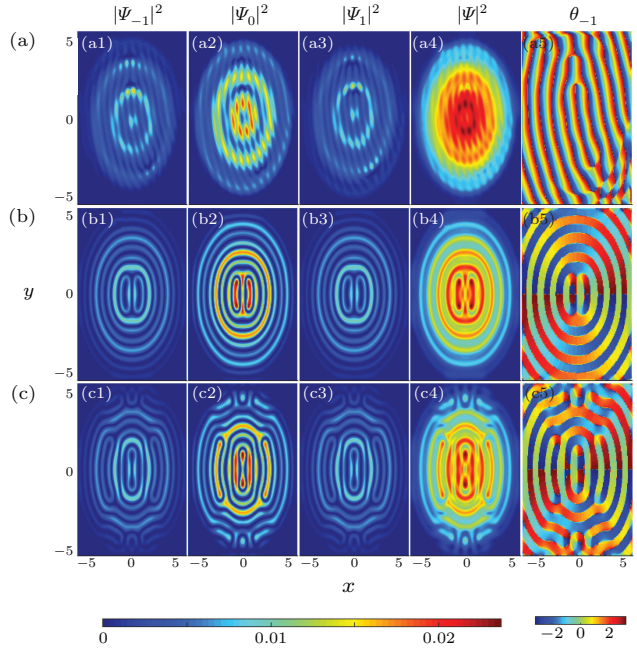



**Fig. 4.** The ground-state density profiles of spin-1 BECs with SOC loaded in a spin-dependent radially periodic potential. The spin-exchange interactions in panels (a)–(c) are $c_2 = -200$, 200, and 2000, respectively. The columns from left to right are the densities of the $m_F = -1$ component, the $m_F = 0$ component, the $m_F = 1$ component, the total component, and the phase of the $m_F = -1$ component. The SOC strength $\gamma = 5$.

## 4. Summary

In summary, we have investigated 2D spin–orbit coupled spin-1 BECs in two types of radially-periodic potentials, *i.e.*, spin-independent and spin-dependent radially-periodic potentials. For the BECs in a spin-independent radially-periodic potential, the density of each component exhibits the periodic density modulation along the azimuthal direction realizes the necklacelike state in the ferromagnetic BECs. As the spin-exchange interaction increases, the necklacelike state gradually transition to the plane wave phase for the antiferromagnetic BECs with larger SOC. The competition of the spin-dependent radially-periodic potential, SOC and spin-exchange interaction gives rise to the exotic ground-state phases when the BECs in a spin-dependent radially-periodic potential.

## References

[1] Ho T L 1998 *Phys. Rev. Lett.* **81** 742
[2] Ohmi T and Machida K 1998 *J. Phys. Soc. Jpn.* **67** 1822
[3] Stoof H T C, Vliegen E and Khawaja U A 2001 *Phys. Rev. Lett.* **87** 120407
[4] Martikainen J P, Collin A and Suominen K A 2002 *Phys. Rev. Lett.* **88** 090404
[5] Ray M W, Ruokokoski E, Kandel S, Möttönen M and Hall D S 2014 *Nature* **505** 657
[6] Ray M W, Ruokokoski E, Tiurev K, Möttönen M and Hall D S 2015 *Science* **348** 544
[7] Wang D S, Song S W, Xiong B and Liu W M 2011 *Phys. Rev A* **84** 053607
[8] Marzlin K P, Zhang W and Sanders B C 2000 *Phys. Rev. A* **62** 013602
[9] Mizushima T, Machida K and Kita T 2002 *Phys. Rev. Lett.* **89** 030401
[10] Leslie L S, Hansen A, Wright K C, Deutsch B M and Bigelow N P 2009 *Phys. Rev. Lett.* **103** 250401
[11] Choi J Y, Kwon W J and Shin Y I 2012 *Phys. Rev. Lett.* **108** 035301
[12] Li Z D, He P B, Li L, Liang J Q and Liu W M 2005 *Phys. Rev. A* **71** 053611
[13] Li L, Li Z D, Malomed B A, Mihalache D and Liu W M 2005 *Phys. Rev. A* **72** 033611
[14] Uchiyama M, Ieda J and Wadati M 2007 *J. Low Temp. Phys.* **148** 399
[15] Nistazakis H E, Frantzeskakis D J, Kevrekidis P G, Malomed B A and Carretero-González R 2008 *Phys. Rev. A* **77** 033612
[16] Xiong B and Gong J B 2010 *Phys. Rev. A* **81** 033618
[17] Li S, Prinari B and Biondini G 2018 *Phys. Rev. E* **97** 022221
[18] Bersano T M, Gokhroo V, Khamehchi M A, Ambroise J D, Frantzeskakis D J, Engels P and Kevrekidis P G 2018 *Phys. Rev. Lett.* **120** 063202
[19] Wang D S, Shi Y R, Feng W X and Wen L 2017 *Physica D* **351–352** 30
[20] Zhao L C, Luo X W and Zhang C W 2020 *Phys. Rev. A* **101** 023621
[21] Lin Y J, Jiménez G K and Spielman I B 2011 *Nature* **471** 83
[22] Wu C and Mondragon S I 2011 *Chin. Phys. Lett.* **28** 097102
[23] Sinha S, Nath R and Santos L 2011 *Phys. Rev. Lett.* **107** 270401
[24] Deng Y, Cheng J, Jing H, Sun C P and Yi S 2012 *Phys. Rev. Lett.* **108** 125301

[25] Hu H, Ramachandhran B, Pu H and Liu X J 2012 *Phys. Rev. Lett.* **108** 010402
[26] Wang J G and Yang S J 2016 *Phys. Rev. A* **93** 043625
[27] Wu Z, Zhang L, Sun W, Xu X T, Wang B Z, Ji S C, Deng Y, Chen S, Liu X J and Pan J W 2016 *Science* **354** 83
[28] Li J, Lee J, Huang W, Burchesky S, Shteynas B, Top F C, Jamison A G and Ketterle W 2017 *Nature* **543** 91
[29] Liu C F and Liu W M 2017 *Opt. Express* **25** 32800
[30] Peng P, Li G Q, Zhao L C, Yang W L and Yang Z Y 2019 *Phys. Lett. A* **383** 2883
[31] Zhu Q L, Pan L H and An J 2020 *Phys. Rev. A* **102** 053320
[32] Wang C J, Gao C, Jian C M and Zhai H 2010 *Phys. Rev. Lett.* **105** 160403
[33] Natu S S, Li X P and Cole W S 2015 *Phys. Rev. A* **91** 023608
[34] Martone G I, Pepe F V, Facchi P, Pascazio S and Stringari S 2016 *Phys. Rev. Lett.* **117** 125301
[35] Campbell D L, Price R M, Putra A, Valdés C A, Trypogeorgos D and Spielman I B 2016 *Nat. Commun* **7** 10897
[36] Sun K, Qu C L, Xu Y, Zhang Y P and Zhang C W 2016 *Phys. Rev. A* **93** 023615
[37] Wang H, Wen L H, Yang H, Shi C X and Li J H 2017 *J. Phys. B* **50** 155301
[38] White A C, Zhang Y P and Busch T 2017 *Phys. Rev. A* **95** 041604
[39] Wang J G, Xu L L and Yang S J 2017 *Phys. Rev. A* **96** 033629
[40] Wang Q B, Yang H, Su N and Wen L H 2020 *Chin. Phys. B* **29** 116701
[41] Han W, Juzeliunas G, Zhang W and Liu W M 2015 *Phys. Rev. A* **91** 013607
[42] Wang J G, Xu L L and Yang S J 2017 *Europhys. Lett.* **120** 20006
[43] Kartashov Y V and Zezyulin D A 2019 *Phys. Rev. Lett.* **122** 123201
[44] Wang Y J, Wen L, Guo H, Tan R B, Zhang S G and Zhang X F 2019 *J. Phys. Soc. Jpn.* **88** 024005
[45] Pan L H, Wu Q, Zhu Q L and Liu Y J 2020 *Phys. Lett. A* **384** 126430
[46] Li J, He T C, Bai J, Liu B and Wang H Y 2021 *Chin. Phys. B* **30** 030302
[47] Bao W, Jaksch D and Markowich P A 2003 *J. Comput. Phys.* **187** 318
[48] Wang H 2007 *Int. J. Comput. Math.* **84** 925